

Fast Channel Estimation and Beam Tracking for Millimeter Wave Vehicular Communications

Sina Shaham, Ming Ding, Matthew Kokshoorn, Zihuai Lin, Xuefeng Yao

School of Electrical and Information Engineering, The University of Sydney, Australia

Email: {sina.shaham, matthew.kokshoorn, zihuai.lin, xuefeng.yao}@sydney.edu.au, ming.ding@data61.csiro.au

Abstract—Millimetre wave (mmWave) is a promising technology to meet the ever-growing data traffic in the future. A major challenge of mmWave communications is the high path loss. In order to overcome this issue, mmWave systems often adopt beamforming techniques, which require robust channel estimation and beam tracking algorithms to maintain an adequate quality of service. This paper proposes a framework of channel estimation and beam tracking for mmWave communications. The proposed framework is designed for vehicular to infrastructure communication but can be extended to other applications as well. First, we propose a multi-stage adaptive channel estimation algorithm called robust adaptive multi-feedback (RAF). The algorithm is based on using the estimated channel coefficient to predict a lower bound for the required number of measurements. Our simulations demonstrate that compared with the existing algorithms, RAF can achieve the desired probability of estimation error (PEE), while on average reducing the feedback overhead by 75.5% and the total channel estimation time by 14%. Second, after estimating the channel in the first step, the paper follows by investigating the extended Kalman filter (EKF) for beam tracking in vehicular communications. A crucial part of EKF is the calculation of Jacobian matrices. We show that the model used in the previous work, which was based on the angles of arrival and departure, is not suitable for vehicular communications. This is due to the complexity in the calculation of Jacobian matrices. A new model is proposed for EKF in mmWave vehicular communications which is based on position, velocity and channel coefficient. Closed-form expressions are derived for the Jacobians used in EKF which facilitate the implementation of the EKF tracking algorithm in the proposed model. Finally, we provide an extensive number of simulations to substantiate the robustness of the framework as well as presenting the analytical results on the PEE of the RAF algorithm.

Index Terms—Millimeter wave, multiple-input multiple-output (MIMO), channel estimation, beamforming, analog beamforming, beam tracking, Extended Kalman filter (EKF).

I. INTRODUCTION

In recent years mobile network operators have been facing a significant growth in data traffic demand. Just in 2016, global data traffic grew 63 percent [1] compared to the previous year. One of the main candidates to address the high data traffic demand of 5G mobile network is millimeter wave (mmWave) wireless communications [2], [3]. The mmWave spectrum is considered to be between 30 to 300 GHz which enables the transmission of higher data rates. Current research in mmWave is mostly focused on the 28 GHz, 38 GHz and 60 GHz bands and also the E-band which comprises 71-76 GHz and 81-86 GHz [4]. Several standards have already been established to regulate the use of mmWave such as ECMA-387 [5], IEEE 802.15.3.c [6], and more importantly, IEEE 802.11ad

[7] which is the first standard in the IEEE 802.11 family to support a mmWave band, i.e., 60 GHz band.

Exploiting the high data rate of mmWave paves the way for a number of exciting applications, such as mmWave cellular systems, vehicle to infrastructure (V2I) and vehicle to vehicle (V2V) communications. The main motivation is the tendency to use the mmWave for applications where a line of sight (LoS) path exists between a transmitter and a receiver. Since the height of a base station is usually much higher than that of vehicles, and embedded transceivers are usually mounted on top of vehicles, it is very likely that LoS communication is available in V2I scenarios which makes mmWave communications well-suited. Some of the practical applications are downloading high-resolution maps for navigation, collecting/distributing aggregated sensor information from/to vehicles which can improve the safety of the drivers and passengers, and also clouding computing of the transmitted data from vehicles. The use of mmWave for vehicular communications is not a new concept, but it is only recently that advancements in CMOS technologies used in radio frequency integrated circuits have made the mmWave products practical. Some initial tests were conducted more than a decade ago [8]. Also, international organization for standardization (ISO) has been working on preliminary standards for mmWave vehicular communications.

A. Beamforming in mmWave

The main difference between mmWave and traditional communication systems is the beamforming techniques required for the channel estimation and beam alignment in mmWave. Communication at high frequencies such as mmWave is well-known for its high path loss which can be understood from the Friis formula [9], indicating that the path loss is inversely proportional to the wavelength of the signal. In spite of the high path loss, since the antenna spacing of antenna arrays is also directly proportional to the wavelength of the signal, the issue of having large path loss in mmWave can be alleviated by increasing the number of antennas packed at the transmitter and receiver, and exploiting their beamforming gain. The problem with this approach lies in the high cost of hardware that prevents the transceiver from utilizing a separate radio frequency (RF) chain for each equipped antenna. This makes fully digital beamforming infeasible for mmWave communications. On the other hand, using an analog-only beamforming also imposes several constraints on engineering and degrades the system performance. The principal idea behind the analog

beamforming is controlling a series of phase shifters with quantized phase and constant modulus using a single RF chain. Analog beamforming limits the processing capability of mmWave transceivers and causes severe issues such as high inter-user interference.

In order to overcome the limitations of analog beamforming and also achieve the good performance of digital beamforming, a new idea of hybrid beamforming is proposed as a reliable solution [10], [11]. In a hybrid architecture, the multiple input multiple output (MIMO) signal process consists of digital precoder and analog precoder. This helps the system to benefit from the robust performance of the digital beamforming and low hardware complexity of the analog beamforming. The precoders are designed independently and then algorithms are applied to optimize the performance [10], [12]. It has been shown that the hybrid beamforming can achieve comparable performance to digital beamforming [10]. A significant advantage of using hybrid architecture is achievement of spatial multiplexing gain which enables the multi-stream and multi-user transmission.

B. Prior Work and Motivation

Adapting mmWave communications to V2I scenarios is challenging. On one hand, having large antenna arrays results in complexity in channel estimation including a large number of feedback bits which reduces the time dedicated for the data transmission. On the other hand, in contrary to the slowly time-variant environments where accurate beam tracking was possible via beam training, fast changing environments such as moving vehicles necessitate the development of new algorithms to track the vehicles. In the following, prior works to tackle the channel estimation and beam tracking in mmWave communications is reviewed.

Recent measurements have demonstrated a sparse nature of mmWave communication channels [13]. Exploiting the sparsity, several works such as [14] and [10] have demonstrated the efficiency of compressed sensing methods in decreasing the training overhead required for the channel estimation. Therefore, channel estimation in mmWave is focused on finding three factors: angle of arrival (AoA), angle of departure (AoD) and channel coefficient (α). Primarily, the authors in [15] proposed a hierarchical multi-resolution beamforming codebook to estimate the channel. In [10], the authors developed a multi-stage adaptive channel estimation algorithm. In each stage, the possible AoA and AoD are divided into two subspaces ($K = 2$), and the most likely subspaces are chosen for further refinement in the next stage. The channel coefficient is estimated after channel estimation is completed. In [16] authors followed the same approach, but used $K = 3$ and also considered the overlapped beam-patterns. One major challenge is that if in any of the stages the estimated angles are incorrect, then the estimation in the following stages will also be incorrect due to the error propagation effect. The authors in [17], developed a rate adaptive algorithm called RACE to ensure that the probability of estimation error (PEE) is below a desired threshold. Unfortunately, the algorithm requires a large number of feedback bits, particularly in low SNR regime.

After channel estimation, in order to prolong the duration of communication between the transmitter and receiver, fast beam tracking methods are required. Authors in [18] proposed a beamforming protocol for 60-GHz propagation channels. The method exploited training sequences for detection of signal strengths. The evaluation of the proposed algorithm was provided in [19]. The approach required multiple beam training whereas our method requires training of only one beam. The most relevant approaches to our work in beam tracking are [20] and [21]. In [20], the focus of the paper is on tracking the beams obtained by a full scan of all possible beam directions. The proposed algorithm applied the EKF to track the paths. This method required a high overhead of pilot transmission to get the measurement matrix. The state model was based on angles and no consideration was given to channel coefficient. In [21], the authors improved the tracking by having a single measurement instead of full scan. The system model was also based on angles and the change in angles was modelled using a Gaussian process noise with zero mean. This assumption is not always valid as it will be shown in this paper. Also, the state evolution model was assumed to be linear which is not the case in most of the vehicular communication systems.

C. Our Contributions

The aim of this paper is to propose a framework for V2I mmWave communication systems which maximize the communication time between the receiver and transmitter. We provide summary of our work in the following.

- We derive the minimum number of feedback bits required for channel estimation ensuring a certain PEE. Then, we propose a new multi-stage adaptive algorithm referred to as Robust Adaptive Multi-Feedback (RAF). The main advantage of the proposed algorithm is its low feedback overhead in mmWave channel estimation.
- We show that the existing model used for beam tracking in mmWave using EKF recursion is not suitable for vehicular communications due to the high complexity in the calculation of Jacobian matrices. Furthermore, we propose new evolution and observation models for beam tracking using EKF recursion, with the derivation of the closed-form expressions for Jacobians.
- We present analytical results on the probability of the estimation error for the proposed RAF algorithm. In more detail, a closed-form upper bound and lower bound have been derived for the PEE.

D. Paper Organization and Notation

The rest of the paper is organized as follows. Section II explains the system model used throughout the paper including channel model, transmission scheme and V2I physical model. Section III introduces the channel estimation algorithm starting by building up the required methods and principles such as channel estimation algorithm with no PEE, sparse representation of the system, maximum likelihood detection method, calculation of optimal feedback bits and finally presenting the RAF algorithm. Section IV describes the proposed beam

tracking technique. Section V provides the simulations and discussions to support the effectiveness of our proposed framework. And finally, section VI presents our conclusion.

Notation : Capital bold-face letter (\mathbf{A}) is used to denote a matrix, \mathbf{a} to denote a vector, a to denote a scalar and \mathcal{A} denotes a set. $\|\mathbf{A}\|^2$ is the magnitude of \mathbf{A} , $|a|$ is the absolute value of a , and determinant is shown by $\det(\mathbf{A})$. \mathbf{A}^T , \mathbf{A}^H and \mathbf{A}^* are the transpose, conjugate transpose and conjugate of \mathbf{A} , respectively. For a square matrix \mathbf{A} , \mathbf{A}^{-1} represents its inverse. \mathbf{I}_N is the $N \times N$ identity matrix and $\lceil \cdot \rceil$ denotes the ceiling function. The superscripts $(\cdot)^R$, $(\cdot)^I$ return real and imaginary parts, respectively. $\mathcal{CN}(\mathbf{m}, \mathbf{R})$ is a complex Gaussian random vector with mean \mathbf{m} and covariance matrix \mathbf{R} , and $\mathbb{E}[a]$ and $\text{Cov}[a]$ denote the expected value and covariance of a , respectively.

II. SYSTEM MODEL

In this section, we present the system model used in the paper. First, we explain the overall structure of mmWave communication system including transmission scheme, physical schematic, and the beamformer structure. Then, we illustrate the channel acquisition model.

A. Structure of mmWave V2I Communication System

1) *Transmission scheme*: The simplified transmission framework and terminology used throughout the paper for communication between the vehicle and BS are summarized in Fig. 1. Beacon interval is defined as the maximum time that data transfer can be conducted before new channel estimation is required. We assume that the beacon interval can be broken into $(m + 1)$ discrete time blocks ($m = 0, \dots, M$). The duration of each block is denoted by Δt . The first block ($m = 0$) starts by channel estimation of vehicle, and the tracking process starts with the following blocks. The channel estimation requires a higher overhead of pilot and feedback bits transmission which necessitates the need for a fast tracking algorithm in order to maximize the data transfer interval. For $m = 1, \dots, M$, each block starts with a single pilot transmission which occupies one time slot. Then, the feedback of the transmitted pilot is received by the transmitter which will be used for the purpose of tracking. Since the duration of channel estimation and slots dedicated to tracking is negligible, the channel is assumed to be static during these slots. This assumption is used in almost all the literature provided for channel estimation such as [16] and [17].

2) *Physical schematic of V2I model*: As illustrated by Fig. 2, a base station (BS) is installed on a cellular tower or building with a height of h . At the transmission block j , a vehicle is assumed to be at the position d_j (point B). Position is defined as the distance of vehicle from the perpendicular line connecting the antenna array to ground. Moreover, the vehicle is assumed to move with a speed of v_j , and having RX angle of θ_j . In the next transmission block, the vehicle has moved to the position d_{j+1} (point C) with the speed and receiving angle of v_{j+1} and θ_{j+1} , respectively. The corresponding TX angles at BS are shown by ϕ_j and ϕ_{j+1} . The TX and RX

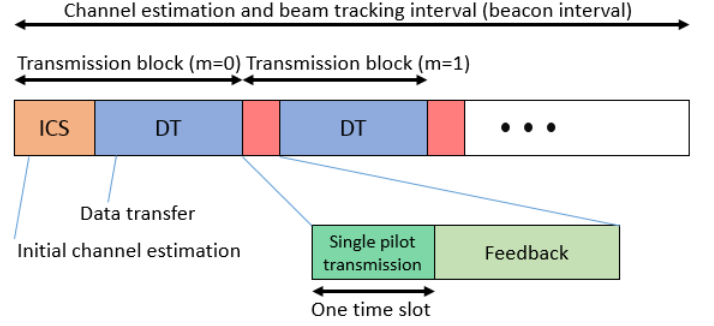


Figure 1: Transmission scheme used for communication between the TX and RX.

angles are chosen to be the angles between the positive x -axis and the line connecting the receiver to the transmitter (BA). Furthermore, the receive antenna array is mounted on the roof-top of the vehicle which results in a dominant LoS path between the transceivers.

3) *Structure of beamformers*: For the proposed framework, we adopt hybrid structure. As proposed by [22]–[24], in hybrid structure, beamforming is divided to a digital precoder followed by an analog precoder. The design of digital precoder for the specifications and codebooks used in our proposed algorithms can be found in [10]. Therefore, we focus on the analog side of the hybrid structure shown in Fig. 3. The proposed framework is explained for a single user, and multi-user scenarios are left for the future work. Hence, we assume a single RF chain at each node. The mmWave communication system is considered to have N_r antennas at the receiver and N_t antennas at the transmitter (TX).

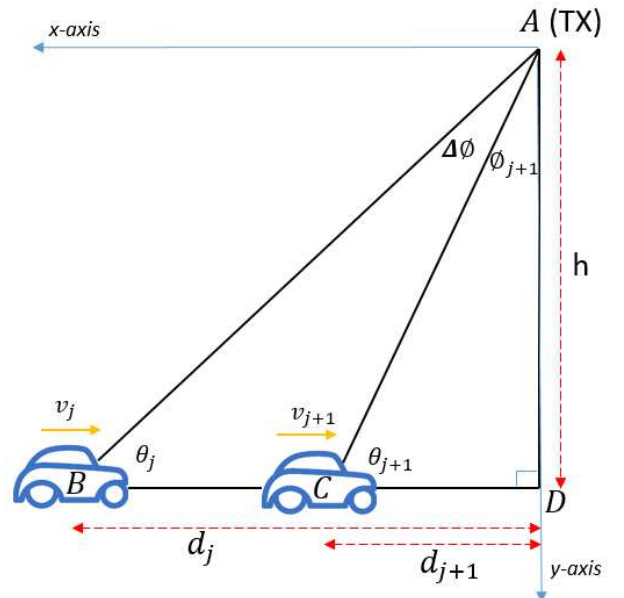


Figure 2: Physical structure of V2I model.

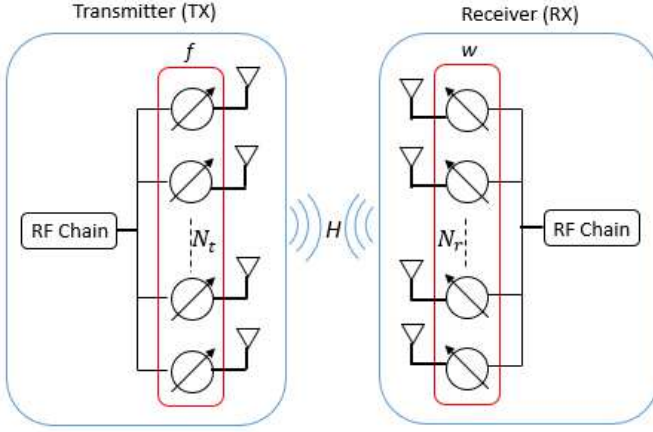


Figure 3: Structure of beamformers.

B. Channel acquisition model

The pilots are assumed to have a unit power and occupy one time slot. If pilot x is transmitted using TX beamformer \mathbf{f} ($\|\mathbf{f}\|^2 = 1$) and power P , the transmitted signal is shown by

$$\mathbf{s} = \sqrt{P}\mathbf{f}x. \quad (1)$$

And at the receiver we observe

$$\mathbf{r}_m = \sqrt{P}\mathbf{H}_m\mathbf{f}x + \mathbf{n}_m, \quad (2)$$

where the subscript m represents the transmission block number and \mathbf{n}_m is a Gaussian process noise ($\mathbf{n}_m \sim \mathcal{CN}(\mathbf{0}, N_0\mathbf{I})$) imposed on the received signal. Furthermore, if the combining vector \mathbf{w} is applied to receive the signal \mathbf{r} , the processed received signal can be written as

$$y_m = \sqrt{P}\mathbf{w}^H\mathbf{H}_m\mathbf{f}x + \mathbf{w}^H\mathbf{n}_m \quad (3)$$

$$= \sqrt{P}\mathbf{w}^H\mathbf{H}_m\mathbf{f}x + n_m. \quad (4)$$

Since $\|\mathbf{w}\|^2 = 1$, n_m follows the same distribution as the elements of the vector \mathbf{n}_m ($n_m \sim \mathcal{CN}(\mathbf{0}, N_0)$).

The AoA and AoD of a single path at m -th transmission block are denoted by θ_m and ϕ_m , respectively. Assuming uniform linear array (ULA) at both ends of the transmission, the receive and transmit array response vectors are given by

$$\mathbf{a}_r(\theta_m) = \frac{1}{\sqrt{N_r}}[1, e^{-j\frac{2\pi}{\lambda}d \cos \theta_m}, \dots, e^{-j(N_r-1)\frac{2\pi}{\lambda}d \cos \theta_m}]^T \quad (5)$$

$$\mathbf{a}_t(\phi_m) = \frac{1}{\sqrt{N_t}}[1, e^{-j\frac{2\pi}{\lambda}d \cos \phi_m}, \dots, e^{-j(N_t-1)\frac{2\pi}{\lambda}d \cos \phi_m}]^T, \quad (6)$$

with d and λ denoting the antenna spacing and the carrier wavelength, respectively. For simplicity, the model is assumed to be in 2D, hence, only azimuth angles are considered. A well-known method which can be used to steer a ULA using phase shifters is progressive phase shift [25]. We adopt a narrowband block-fading channel model for the communication system. Therefore, \mathbf{H}_m which is an $N_r \times N_t$ matrix representing the channel between the RX and TX can be written as

$$\mathbf{H}_m = \sum_{l=1}^L \alpha_m^{(l)} \mathbf{a}_r(\theta_m^{(l)}) \mathbf{a}_t(\phi_m^{(l)})^H, \quad (7)$$

where the index l implies the l -th path and $\alpha_m^{(l)}$ represents the complex path gain of the path. Scattering in mmWave induces more than 20dB attenuation [26]. Hence, we consider LoS component as the target path for the channel estimation and tracking of the vehicle. This is a reasonable assumption as it is shown that almost only LoS component can provide the reliability for the high transmission rate in mmWave communications [26], [27]. Moreover, recent measurements have shown the mmWave to be sparse in the geometric domain [28]. Hence, paths are more likely to be separated and we can assume that only one path lies within the main beam direction [29]. The other paths are assumed to fall into the sidelobes. Therefore, we consider non-LoS paths to be negligible compared to the more dominant LoS component. This assumption becomes more accurate as the number of antennas increases and the beamwidth grows narrower. Thus, the observed signal from equation (4) is given by

$$y_m = \sqrt{P}\alpha_m \mathbf{w}^H \mathbf{a}_r(\theta_m) \mathbf{a}_t(\phi_m)^H \mathbf{f}x + n_m. \quad (8)$$

Since we explain our framework for one beacon interval and the channel estimation is only conducted once in a beacon at m equal to zero, to simplify the notation, we drop the subscript zero for the channel estimation and represent the observed pilot as

$$y = \sqrt{P}\alpha \mathbf{w}^H \mathbf{a}_r(\theta) \mathbf{a}_t(\phi)^H \mathbf{f}x + n. \quad (9)$$

Starting from $m = 1$, transceivers will have the estimated AoA and AoD. Therefore, the pointing direction of the beamformers is adjusted to these angles. Denoting the pointing direction of the receiver combiner and the transmit beamformer at the m -th transmission block by $\bar{\theta}_m$ and $\bar{\phi}_m$, the directed beamformers can be shown as

$$\mathbf{w}(\bar{\theta}_m) = \frac{1}{\sqrt{N_r}}[1, e^{-j\frac{2\pi}{\lambda}d \cos \bar{\theta}_m}, \dots, e^{-j(N_r-1)\frac{2\pi}{\lambda}d \cos \bar{\theta}_m}]^T \quad (10)$$

$$\mathbf{f}(\bar{\phi}_m) = \frac{1}{\sqrt{N_t}}[1, e^{-j\frac{2\pi}{\lambda}d \cos \bar{\phi}_m}, \dots, e^{-j(N_t-1)\frac{2\pi}{\lambda}d \cos \bar{\phi}_m}]^T. \quad (11)$$

which result in the observed signal of

$$y_m = \sqrt{P}\alpha_m \mathbf{w}(\bar{\theta}_m)^H \mathbf{a}_r(\theta_m) \mathbf{a}_t(\phi_m)^H \mathbf{f}(\bar{\phi}_m)x + n_m. \quad (12)$$

III. THE PROPOSED CHANNEL ESTIMATION ALGORITHM

Communication between the TX and RX starts by estimating the channel. Here, we propose an algorithm called RAF which significantly reduce the duration of channel estimation, making it a viable algorithm for V2I scenarios. First, extended version of the binary search algorithm represented in [10] is explained. In this algorithm, no consideration has been made on PEE requirement. Then, a sparse representation of the system is developed followed by a method called MLD which

is used for the purpose of detection of the AoA and AoD. In the next step, the answer will be given on what the optimal number of feedback bits is to ensure the PEE and finally, the pieces are put together by explaining our proposed algorithm RAF.

A. Multi-stage Channel Estimation Algorithm with no PEE Constraint

Extending the approach in [10], during each stage, possible AoAs and AoDs are divided into K sub-spaces creating K^2 combination. The target path is located in one of the candidate pairs of angle sub-spaces and will be estimated. After estimating the sub-spaces, they are further divided into another K sub-spaces. The process continues until the AoD and AoA reach the specified resolution. In the s -th stage, the beamforming vectors at the TX and RX for the k -th sub-space are represented by \mathbf{f}_k^s and \mathbf{w}_k^s . The estimation of sub-spaces is explained in the following.

A pilot signal ($|x|^2 = 1$) is sent in each of the K^2 transmitter and receiver angle combinations where each combination corresponds to one AoA subspace candidate at the receiver and one AoD subspace candidate at the transmitter. Therefore, the system can be represented as

$$\mathbf{c}^{s,K^2} = \sqrt{P}x\mathbf{l}^{s,K^2} + \mathbf{n}^{s,K^2}, \quad (13)$$

where superscripts represent the stage number and number of measurements, \mathbf{n} is $K^2 \times 1$ vector of i.i.d white Gaussian noise random variables, and \mathbf{l}^{s,K^2} is a vector containing the channel response to all the combinations of transmit and receive beamforming vectors,

$$\mathbf{l}^{s,K^2} = \begin{bmatrix} (\mathbf{w}_1^s)^H \mathbf{H} \mathbf{f}_1^s \\ (\mathbf{w}_2^s)^H \mathbf{H} \mathbf{f}_1^s \\ \vdots \\ (\mathbf{w}_1^s)^H \mathbf{H} \mathbf{f}_2^s \\ (\mathbf{w}_2^s)^H \mathbf{H} \mathbf{f}_2^s \\ \vdots \\ (\mathbf{w}_K^s)^H \mathbf{H} \mathbf{f}_K^s \end{bmatrix}. \quad (14)$$

In order to find the desired beamforming vectors, the dictionary matrix of all the possible steering vectors for the angles is written as

$$\mathbf{A}_{\text{DIC}} = [\mathbf{a}(0), \mathbf{a}(\frac{2\pi}{N_t}), \dots, \mathbf{a}(\frac{2\pi(N_t-1)}{N_t})]. \quad (15)$$

Finding the beamforming vector for the k th sub-range at the TX is done by solving

$$\mathbf{A}_{\text{DIC}}^H \mathbf{f}_k^s = \mathbf{z}^{s,k}, \quad (16)$$

where $\mathbf{z}^{s,k}$ is an $N_t \times 1$ vector in which the values included in the intended transmit subrange are equal to the constant C_s and zero otherwise. The value of C_s is chosen to make the magnitude of the beamforming vectors equal to one ($\|\mathbf{f}\|^2 = 1$). From equation (16), \mathbf{f}_k^s is calculated as

$$\mathbf{f}_k^s = (\mathbf{A}_{\text{DIC}} \mathbf{A}_{\text{DIC}}^H)^{-1} \mathbf{A}_{\text{DIC}} \mathbf{z}^{s,k}. \quad (17)$$

The same procedure is used to find the beamforming vectors of the RX. After K^2 measurement, the RX will compare the magnitude of K^2 received pilots and choose the one with the largest magnitude which is likely to be the desired path.

Although this algorithm is able to estimate the channel, there is no procedure to ensure the desired PEE. Therefore, it is necessary to extend the algorithm in order to reduce the error in each stage below the specified threshold.

B. A Sparse Representation of the System

In stage s , the explained multi-stage channel estimation algorithm conducts K^2 measurements, therefore, substituting \mathbf{H} into equation (14), we have

$$\mathbf{l}^{s,K^2} = \alpha \begin{bmatrix} (\mathbf{w}_1^s)^H \mathbf{a}_r(\theta) \mathbf{a}_t(\phi)^H \mathbf{f}_1^s \\ (\mathbf{w}_2^s)^H \mathbf{a}_r(\theta) \mathbf{a}_t(\phi)^H \mathbf{f}_1^s \\ \vdots \\ (\mathbf{w}_1^s)^H \mathbf{a}_r(\theta) \mathbf{a}_t(\phi)^H \mathbf{f}_2^s \\ (\mathbf{w}_2^s)^H \mathbf{a}_r(\theta) \mathbf{a}_t(\phi)^H \mathbf{f}_2^s \\ \vdots \\ (\mathbf{w}_K^s)^H \mathbf{a}_r(\theta) \mathbf{a}_t(\phi)^H \mathbf{f}_K^s \end{bmatrix} \quad (18)$$

The multiplication of $(\mathbf{w}_1^s)^H \mathbf{a}_r(\theta)$ and $\mathbf{a}_t(\phi)^H \mathbf{f}_1^s$ is only non-zero if the AoA and AoD are aligned to the beamforming vectors. Therefore, only one row of \mathbf{l}^{s,K^2} is non-zero [10]. A new matrix $\mathbf{G}^{s,q}$ at its initial state is defined as

$$\mathbf{G}^{s,q} = \mathbf{G}^{s,K^2} = \mathbf{I}_{K \times K}, \quad (19)$$

The index q used in the notation denotes the number of measurements conducted so far. The superscript q is necessary since there will be a larger number of measurements to ensure the PEE.

Finding the AoA and AoD is equivalent to finding a $K^2 \times 1$ vector \mathbf{v} which is zero everywhere except the desired row of $\mathbf{G}^{s,q}$ where it is equal to one. Hence, $\mathbf{l}^{s,q}$ and the observation vector can be written as

$$\mathbf{l}^{s,q} = \sqrt{P}x C_s^2 \alpha \mathbf{G}^{s,q} \mathbf{v}^T \quad (20)$$

$$\mathbf{c}^{s,q} = \sqrt{P}x C_s^2 \alpha \mathbf{G}^{s,q} \mathbf{v}^T + \mathbf{n}^q. \quad (21)$$

Assuming element d of \mathbf{v} is one, the estimated AoA subspace \hat{k}_t and the AoD subspace \hat{k}_r are calculated by

$$\hat{k}_t = \lceil \frac{d}{K} \rceil, \quad \hat{k}_r = d - K(\hat{k}_t - 1). \quad (22)$$

The new presentation of the system indicates that the possible outcomes of the channel estimation are equivalent to the rows of matrix $\mathbf{G}^{s,q}$.

C. Maximum Likelihood Detection (MLD)

In our algorithm, the MLD method will be used for the estimation of AoA and AoD. After q measurements, the distribution of observation vector $\mathbf{c}^{s,q}$ can be written as

$$\mathbf{c}^{s,q} = \mathcal{CN}(0, \mathbf{\Sigma}_v), \quad (23)$$

where

$$\Sigma_v = PC_s^4 G^{s,q} v v^T (G^{s,q})^H + N_0 I_q. \quad (24)$$

We refer to [16] for the derivation. It can be seen that the received vector follows circularly symmetric complex Gaussian (CSCG) distribution which has the distribution of

$$f(\mathbf{c}^{s,q} | \mathbf{v}, \mathbf{G}^{s,q}) = \frac{1}{\pi^q \det(\Sigma_v)} \exp(-(\mathbf{c}^{s,q})^H \Sigma_v^{-1} \mathbf{c}^{s,q}). \quad (25)$$

In order to get a better understanding of the density, it is useful to see them in terms of probability. Defining the set \mathcal{V} as all possible K^2 outcomes of the vector \mathbf{v} , the probability can be written as

$$p(\mathbf{v} | \mathbf{c}^{s,q}) = \frac{f(\mathbf{c}^{s,q} | \mathbf{v})}{\sum_{\mathbf{j} \in \mathcal{V}} f(\mathbf{c}^{s,q} | \mathbf{j})}. \quad (26)$$

We are looking for the vector \mathbf{j} which results in maximum probability ($\arg\max_{\mathbf{j} \in \mathcal{V}} p(\mathbf{v} | \mathbf{c}^{s,q})$), which then, as explained in the previous section can be used to find the AoA and AoD. Upon completion of the final stage S , the channel coefficient is estimated as

$$\hat{\alpha} = \frac{x(\mathbf{w}_{\hat{k}_r}^S)^H \mathbf{H} \mathbf{f}_{\hat{k}_t}^S}{C_s^2}. \quad (27)$$

D. The Optimal Number of Feedback to Achieve the PEE

In order to have a benchmark to compare the RAF algorithm's feedback performance, it is important to know what the optimal number of feedback bits is. Note that the number has to ensure the desired PEE. In other words, we are looking for the minimum implementable feedback number that guarantees the desired PEE. From information theory, the minimum number is one with a single feedback including $\lceil \log_2(K) \rceil$ bits [30]. We verify that this number is actually achievable by developing an algorithm which only needs $\lceil \log_2(K) \rceil$ bits of feedback. The cost of having the optimal number of feedback bits is a large number of channel measurements. Therefore, this algorithm is just used as a benchmark and can not be a good alternative in practice.

We denote Γ as the probability of the event that a channel estimation is incorrect. The algorithm starts by having the initial K^2 measurements which result in the primary channel estimation. The TX continues to send the pilots using the same sequence as the initial measurements. After each transmission, using MLD the RX calculates $p(\mathbf{v} | \mathbf{c}^{s,q})$. As soon as reaching the desired PEE ($p(\mathbf{v} | \mathbf{c}^{s,q}) > (1 - \Gamma)$) the RX will feedback $\lceil \log_2(K) \rceil$ bits to notify the TX about the estimated AoD. The process of adding a new measurement for the TX subspace of \hat{k}_t and the RX subspace of \hat{k}_r is written mathematically as

$$\mathbf{c}^{s,q+1} = \sqrt{P}x \left[(\mathbf{w}_{\hat{k}_r}^s)^H \mathbf{H} \mathbf{f}_{\hat{k}_t}^s \right] + \left[(\mathbf{w}_{\hat{k}_r}^s)^H \mathbf{n} \right], \quad (28)$$

Note that there is always a probability of 'outage' when the channel coefficient is close to zero. In order to prevent the

Algorithm 1: An algorithm which requires the optimal number of feedback bits.

```

1 Input:  $N_t, N_r, K$ .
2 Initialization: .
3 for  $s < S$  do
4   // Calculate:
5    $\{\mathbf{f}_k^s\} \quad \forall k = 1, \dots, K$ 
6    $\{\mathbf{w}_k^s\} \quad \forall k = 1, \dots, K$ 
7   for  $i = 1$  to  $K$  do
8     for  $j = 1$  to  $K$  do
9       Transmitter transmits using  $\mathbf{f}_i^s$ 
10      Receiver measures using  $\mathbf{w}_j^s$ 
11    end
12  end
13  // After initial  $K^2$  measurements
14   $q = K^2$ 
15   $\mathbf{c}^{s,q} = \sqrt{P}x \mathbf{t}^{s,q} + \mathbf{n}^{s,q}$ 
16   $\mathbf{d} = \arg\max_{\mathbf{j} \in \mathcal{V}} p(\mathbf{v} | \mathbf{c}^{s,q})$ 
17   $\mathbf{d} \leftarrow$  non-zero element of  $\mathbf{d}$ 
18   $\hat{k}_t = \lceil \frac{d}{K} \rceil, \hat{k}_r = d - K(\hat{k}_t - 1)$ 
19  while  $p(\mathbf{v} | \mathbf{c}^{s,q}) < (1 - \Gamma)$  and  $q < q_{\max}$  do
20     $q = q + 1$ 
21    Transmitter transmits using  $\mathbf{f}_{\hat{k}_t}^S$ 
22    Receiver receives using  $\mathbf{w}_{\hat{k}_r}^S$ 
23    // Update:
24     $\mathbf{d} = \arg\max_{\mathbf{j} \in \mathcal{V}} p(\mathbf{v} | \mathbf{c}^{s,q})$ 
25     $\mathbf{d} \leftarrow$  non-zero element of  $\mathbf{d}$ 
26     $\hat{k}_t = \lceil \frac{d}{K} \rceil, \hat{k}_r = d - K(\hat{k}_t - 1)$ 
27  end
28 end
29 Output:  $\hat{\alpha} = \frac{x(\mathbf{w}_{\hat{k}_r}^S)^H \mathbf{H} \mathbf{f}_{\hat{k}_t}^S}{C_s^2}, \hat{k}_t, \hat{k}_r$ .
```

excessive number of measurement, we set a maximum to the number of pilots which could be transmitted denoted by q_{\max} . The formal representation of the algorithm is given in Alg. 1.

E. Robust Adaptive Multi-feedback Algorithm (RAF)

Multi-stage channel estimation algorithms are mainly based on a fixed number of channel estimation. As an example, the authors in [10] used K^2 measurements in each stage to estimate the channel. Although the proposed algorithms are effective, they did not consider the performance in terms of the PEE. If due to the additive noise, the detection of the estimated AoA and AoD is incorrect in any of the stages, the algorithms will not be able to estimate the channel correctly. Therefore, devising an algorithm to ensure the PEE is crucial. The authors in [17], proposed a rate adaptive algorithm (RACE) in order to reach the desired PEE. Unfortunately, the algorithm requires a high number of channel feedback even for $K = 2$, particularly in low SNR. Therefore, it is not possible to use the algorithm in fast changing environments such as V2I scenarios. We propose an algorithm called RAF. In contrary to the existing

algorithms, RAF exploits the estimated channel coefficient. The significance of using channel coefficient is the entailed information about the number of measurements required. This helps to estimate the time to commence sending the feedback and consequently requires a low number of feedback bits as well as pilot transmissions.

Before explaining the algorithm, we use information theory to find a lower bound for the number of measurements. The channel estimation is equivalent to finding a vector \mathbf{v} which contains K^2 binary bits encoded into q (number of pilots transmitted) symbols. Therefore, the system has a transmission rate of $\mathcal{C} = \frac{K^2}{q}$. According to the Shannon-Hartley theorem [30]

$$\mathcal{C} = \frac{K^2}{q} \leq \log_2(1 + SNR_s) \quad (29)$$

$$\rightarrow q \geq \frac{K^2}{\log_2(1 + SNR_s)}, \quad (30)$$

where SNR_s (in stage s) can be written as

$$SNR_s = \frac{|\alpha|^2 PK^{(2s-2)}}{N_0}. \quad (31)$$

Substituting equation (31) in (30), a lower bound can be found for the number of measurements that are required in each stage on condition of the estimated value of α . After q measurements ($q \geq K^2$), if the mean of observations received in the estimated AoA and AoD are denoted by λ^q , the value of α can be estimated as

$$\hat{\alpha} = \frac{\lambda^q}{\sqrt{PC_s^2}}. \quad (32)$$

Therefore, we have a lower bound for the number of measurements required.

In each stage, the RAF algorithm starts by conducting K^2 initial channel measurements. The MLD enables the system to have an estimation of the AoA and AoD which can be used to estimate the value of channel coefficient (α). Having the estimated α , the receiver can predict a lower bound for the required number of measurements. Up to the point of reaching the PEE threshold, the TX continues to send the pilots as explained in the optimal feedback algorithm. As the pilots are accumulated, the same process of MLD is used to achieve a better estimation of α which results in obtaining a more accurate lower bound. After reaching the PEE threshold, the RX feeds back the estimated AoD. At this point, the TX stops sending the pilots in the order of initial channel estimation and only sends a pilot in the estimated AoD. The RX knows the estimated AoA and utilizes the corresponding combiner to receive the pilot. Following the same process after receiving each pilot, the RX estimates the AoA and AoD and feeds back the estimated AoD. The stage terminates as soon as the required estimation precision is reached. In the final transmission of feedback bits, an extra bit will be transmitted to notify the transmitter to stop the transmission of pilot signals. The RAF algorithm is represented formally in Alg. 2.

Algorithm 2: Robust adaptive multi-feedback algorithm (RAF).

```

1 Input:  $N_t, N_r, K$ .
2 Initialization: .
3 for  $s < S$  do
4   // Calculate:
5    $\{\mathbf{f}_k^s\} \quad \forall k = 1, \dots, K$ 
6    $\{\mathbf{w}_k^s\} \quad \forall k = 1, \dots, K$ 
7   for  $i = 1$  to  $K$  do
8     for  $j = 1$  to  $K$  do
9       Transmitter transmits using  $\mathbf{f}_i^s$ 
10      Receiver measures using  $\mathbf{w}_j^s$ 
11    end
12  end
13  // After initial  $K^2$  measurements
14   $q = K^2$ 
15   $\mathbf{c}^{s,q} = \sqrt{P} \mathbf{x} \mathbf{I}^{s,q} + \mathbf{n}^{s,q}$ 
16   $\mathbf{d} = \underset{j \in \mathcal{V}}{\operatorname{argmax}} p(\mathbf{v} | \mathbf{c}^{s,q})$ 
17   $\mathbf{d} \leftarrow$  non-zero element of  $\mathbf{d}$ 
18   $\hat{k}_t = \lceil \frac{d}{K} \rceil$ ,  $\hat{k}_r = d - K(\hat{k}_t - 1)$ 
19  // Find a lower bound for the number of
    measurements required
20   $\lambda^q \leftarrow$  the mean of values in  $\mathbf{c}^{s,q}$  corresponding to  $\hat{k}_t$ 
    and  $\hat{k}_r$ 
21   $\hat{\alpha} = \frac{\lambda^q}{\sqrt{PC_s^2}}$ 
22   $L \leftarrow \frac{K^2}{\log_2(1 + \frac{|\hat{\alpha}|^2 PK^{(2s-2)}}{N_0})}$ 
23  for  $i = 1$  to  $K$  do
24    for  $j = 1$  to  $K$  do
25       $q = q + 1$ 
26      Transmitter transmits using  $\mathbf{f}_i^s$ 
27      Receiver measures using  $\mathbf{w}_j^s$ 
28      Repeat lines 20 to 22
29      if  $q \geq L$  then
30        Break;
31      end
32    end
33    if  $q \geq L$  then
34      Break;
35    end
36  end
37  // Update:
38  Repeat lines 16 to 18
39  while  $p(\mathbf{v} | \mathbf{c}^{s,q}) < (1 - \Gamma)$ 
40     $q < q_{\max}$  do
41       $q = q + 1$ 
42      Transmitter transmits using  $\mathbf{f}_{\hat{k}_t}^s$ 
43      Receiver receives using  $\mathbf{w}_{\hat{k}_r}^s$ 
44      // Update:
45      Repeat lines 16 to 18
46    end
47  end
48 Output:  $\hat{\alpha} = \frac{x(\mathbf{w}_{\hat{k}_r}^s)^H \mathbf{H} \mathbf{f}_{\hat{k}_t}^s}{C_s^2}$ ,  $\hat{k}_t$ ,  $\hat{k}_r$ .
```

IV. THE PROPOSED BEAM TRACKING ALGORITHM

In this section, the proposed system model for EKF algorithm is explained. First, the necessity for a new state evolution model is demonstrated, followed by the proposed model. Then, the observation model corresponding to the state evolution model is derived, and finally, the EKF algorithm is illustrated.

A. State Evolution Model

Previous attempts at applying the EKF algorithm on mmWave beam tracking [29], [20] were based on using the AoA and AoD as state variables. The used state evolution model was linear and assumed to evolve by a Gaussian noise with zero mean. Also, the noise was additive which highly simplified the equations. Unfortunately, such modeling is not realistic for most of the vehicular communication scenarios. This becomes evident considering how actually the angles evolve in Fig 2.

Lemma 1. *If a vehicle moves from the transmit angle ϕ_j to ϕ_{j+1} , the change in the transmit angle and similarly for the receiving angle can be calculated by*

$$\phi_{j+1} - \phi_j = -\cot^{-1}\left(\frac{h}{\cos^2\phi_j(v_j + w_j)\Delta t} - \tan\phi_j\right), \quad (33)$$

where v_j is the velocity of the vehicle at the first location and w_j is the Gaussian noise.

Proof. Considering Fig. 2 and denoting the length of the line AC by T , we write the sines rule [31] in triangles ABC and ACD . Therefore, we have

$$\frac{\Delta d}{\sin(\Delta\phi)} = \frac{T}{\sin(90 - \phi_j)} \quad (34)$$

and

$$\frac{T}{\sin(90)} = \frac{h}{\sin(90 - \phi_{j+1})}. \quad (35)$$

Substituting T from equation (35) into (34), the Δd is derived as

$$\Delta d = \frac{\sin(\Delta\phi)h}{\cos(\phi_j)\cos(\phi_{j+1})}. \quad (36)$$

Furthermore, $\cos(\phi_{j+1})$ can be written as

$$\begin{aligned} \cos(\phi_{j+1}) &= \cos(\phi_{j+1} - \phi_j + \phi_j) \\ &= \cos(\Delta\phi)\cos(\phi_j) + \sin(\Delta\phi)\sin(\phi_j) \end{aligned} \quad (37)$$

and by substituting it into equation (36), the Kinematic formula relating the velocity to displacement is derived as

$$\begin{aligned} \Delta d &= (v_j + w_j)\Delta t \\ &= \frac{\sin(\Delta\phi)h}{\cos(\phi_j)(\cos(\Delta\phi)\cos(\phi_j) + \sin(\Delta\phi)\sin(\phi_j))}. \end{aligned} \quad (38)$$

Solving equation (38) for $\Delta\phi$ results in the equation (33). \square

Recall that the main drawback of EKF is the complexity in its implementation. It can be seen that equation (33) is non-linear with respect to the angle. Also, the process noise which happens due to the change in velocity is non-additive. These

are the two main factors affecting the complexity. Therefore, if we are to use the angles as state variables, the calculation of the Jacobians for EKF algorithm is of high complexity. Here, we propose to use the position, velocity and complex channel gain as the state variables which give a linear state model and additive process noise for vehicular communications. As a result, the state vector can be written as

$$\mathbf{x}_m = [d_m, v_m, \alpha_m^R, \alpha_m^I]^T, \quad (39)$$

where d_m and v_m denote the position and velocity of the vehicle at the m -th transmission block, respectively. The Gaussian coefficient is divided into a real part and an imaginary part, i.e., $\alpha_m = \alpha_m^R + j\alpha_m^I$ which helps to have the state vector as real numbers. α_m^R and α_m^I are assumed to follow the first order Gauss-Markov model [29] expressed by

$$\alpha_{m+1}^R = \rho\alpha_m^R + \xi_m \quad (40)$$

$$\alpha_{m+1}^I = \rho\alpha_m^I + \xi'_m, \quad (41)$$

where ρ is the correlation coefficient, $\xi_m, \xi'_m \sim \mathcal{N}(0, \frac{1-\rho^2}{2})$, and $\xi[-1], \xi'_[-1] \sim \mathcal{N}(0, \frac{1}{2})$. The evolution of position and velocity are thus formulated as

$$d_{m+1} = d_m + v_m\Delta t + w_m\Delta t \quad (42)$$

$$v_{m+1} = v_m + w_m, \quad (43)$$

with w_m denoting the process noise which represents the change in the speed of the vehicle. It is assumed to follow Gaussian distribution $w_m \sim \mathcal{N}(0, \sigma_w^2)$. In summary, the state evolution equation can be written as

$$\mathbf{x}_{m+1} = \mathbf{A}\mathbf{x}_m + \mathbf{u}_m, \quad (44)$$

where

$$\mathbf{A} = \begin{bmatrix} 1 & \Delta t & 0 & 0 \\ 0 & 1 & 0 & 0 \\ 0 & 0 & 1 & 0 \\ 0 & 0 & 0 & 1 \end{bmatrix}, \quad (45)$$

and $\mathbf{u}_m \sim \mathcal{N}(0, \Sigma_u)$ with

$$\Sigma_u = \text{diag}([(\Delta t\sigma_w)^2, (\sigma_w)^2, 1 - \rho^2, 1 - \rho^2]). \quad (46)$$

B. The Observation Expression

In order to complete the model for the EKF algorithm, we need to derive the measurement function in terms of the state variables. By substituting the equations (5,6,10,11) in the observation equation (12) we have

$$\begin{aligned} y_m &= \frac{\sqrt{P}\alpha_m x}{N_t N_r} \left(\sum_{p=0}^{N_t-1} e^{-j\frac{2\pi}{\lambda} dp(\cos\theta_m - \cos\bar{\theta}_m)} \right) \times \\ &\quad \left(\sum_{q=0}^{N_t-1} e^{j\frac{2\pi}{\lambda} dq(\cos\phi_m - \cos\bar{\phi}_m)} \right) + n_m \\ &= \frac{\sqrt{P}\alpha_m}{N_t N_r} \sum_{q=0}^{N_t-1} \sum_{p=0}^{N_t-1} e^{j\frac{2\pi}{\lambda} d(-p\cos\theta_m + q\cos\phi_m + b_{pq})} + n_m, \end{aligned} \quad (48)$$

$$\frac{\partial y_m}{\partial d_m} = \sum_{q=0}^{N_t-1} \sum_{p=0}^{N_r-1} \frac{\frac{\sqrt{P}\alpha_m x}{N_t N_r} j \frac{2\pi}{\lambda} dh^2(p+q)}{\sqrt{(h^2 + (d_{m-1} + v_{m-1}\Delta t)^2)^3}} \times \frac{j \frac{2\pi}{\lambda} d(b_{pq} \sqrt{h^2 + (d_{m-1} + v_{m-1}\Delta t)^2} + (p+q)(d_{m-1} + v_{m-1}\Delta t))}{\sqrt{h^2 + (d_{m-1} + v_{m-1}\Delta t)^2}} \quad (47)$$

where

$$b_{pq} = p \cos \bar{\theta}_m - q \cos \bar{\phi}_m. \quad (49)$$

In Fig. 2, the AoA and AoD of the system can be measured as

$$\theta_m = \text{atan2}\left(\frac{-h}{-d_m}\right) = \text{atan2}\left(\frac{-h}{-(d_{m-1} + v_{m-1}\Delta t)}\right) \quad (50)$$

$$\phi_m = \text{atan2}\left(\frac{h}{d_m}\right) = \text{atan2}\left(\frac{h}{d_{m-1} + v_{m-1}\Delta t}\right). \quad (51)$$

where atan2 is the four-quadrant inverse tangent. The cosine of the angles are calculated as ¹

$$\cos(\theta_m) = \frac{-(d_{m-1} + v_{m-1}\Delta t)}{\sqrt{h^2 + (d_{m-1} + v_{m-1}\Delta t)^2}} \quad (52)$$

$$\cos(\phi_m) = \frac{(d_{m-1} + v_{m-1}\Delta t)}{\sqrt{h^2 + (d_{m-1} + v_{m-1}\Delta t)^2}} \quad (53)$$

Substituting equations (52), (53) into (48), we have the observation equation in terms of the state variables as

$$y_m = \frac{\sqrt{P}\alpha_m x}{N_t N_r} \times \sum_{q=0}^{N_t-1} \sum_{p=0}^{N_r-1} e^{j \frac{2\pi}{\lambda} d \left(\frac{(p+q)(d_{m-1} + v_{m-1}\Delta t)}{\sqrt{h^2 + (d_{m-1} + v_{m-1}\Delta t)^2}} + b_{pq} \right)} \quad (54)$$

$$+ n_m = g(\mathbf{x}_m) + n_m.$$

C. EKF based beam tracking

In this subsection, we will present how to use the EKF to track the vehicle. As the vehicle moves, the state vector of the process evolves. Our aim is to match the $\bar{\theta}_m$ and $\bar{\phi}_m$ to θ_m and ϕ_m , respectively.

EKF recursion [32] is described in the Fig. 4. For estimating the state at the $(m+1)$ -th transmission block, the algorithm starts by assigning the predicted values of $(m+1)$ -th state estimate and its covariance to the values of m -th transmission block. Then, the Kalman gain is calculated based on the assigned values. Finally, obtaining a new observation and using the values calculated for Kalman gain, the $(m+1)$ -th state and its covariance are updated. In Fig. 4, \mathbf{C}_{m+1} is the observation transition matrix defined by the following Jacobian matrix

$$\mathbf{C}_{m+1} = \left. \frac{\partial g}{\partial \mathbf{x}} \right|_{\hat{\mathbf{x}}_{m+1|m}}. \quad (55)$$

¹ $\cos(\text{atan2}(\frac{y}{x})) = \frac{y}{\sqrt{x^2 + y^2}}.$

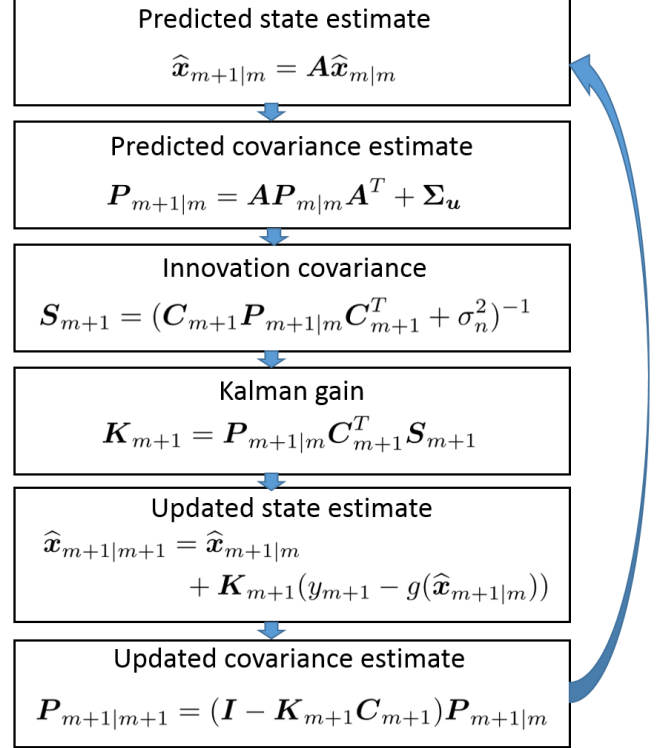


Figure 4: Flowchart of EKF recursion.

The partial derivative with respect to position is given in the equation (47) and the partial derivative with respect to velocity is calculated by

$$\frac{\partial y_m}{\partial v_m} = \frac{\partial y_m}{\partial d_m} \times \Delta t. \quad (56)$$

For the channel coefficient, calculation of the partial derivative is straightforward (equation (47) excluding noise and channel coefficient). Note that in order to deal with real numbers in implementation of the EKF, y_m and \mathbf{C}_m are substituted by $\tilde{y}_m = [y_m^R, y_m^I]^T$ and $\tilde{\mathbf{C}}_m = [\mathbf{C}_m^R, \mathbf{C}_m^I]^T$ in the equations used in the Fig. 4.

V. SIMULATION RESULTS AND DISCUSSIONS

In this section, we start by explaining the simulation set up of our system followed by a comprehensive analysis of channel estimation based on the PEE and overall estimation time. Then, we focus on efficiency of the proposed beam tracking model and various factors affecting its performance. Finally, the impact of channel estimation error on tracking is investigated.

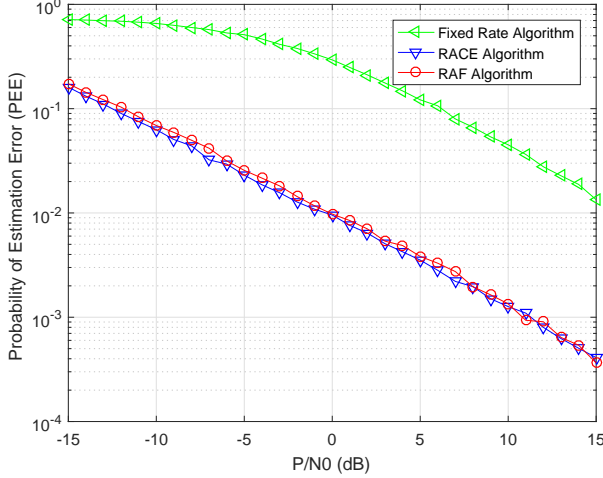


Figure 5: Performance of the RAF algorithm compared to the algorithms in [17] and [10] in terms of PEE.

A. Simulation Setup

The system is assumed to have 64 antennas at both TX and RX spaced by $\lambda/2$. The channel coefficient is assumed to follow a Gaussian distribution with zero mean and unit covariance ($\mathcal{CN}(0,1)$). The initial AoD and AoA are set to -135 and 45 degrees. Besides, we assume that $\rho = 0.995$, $\Delta t = .001s$, the tower height $h = 3m$, the initial speed of the vehicle is $60km/h$ and the variation in the speed of vehicle is set to $\sigma_w = 1.4m/s$.

Since the channel estimation algorithms have the same number of stages and follow the same process in each one, we compare the algorithms in a single stage which helps to reduce the simulation complexity. Moreover, in order to compare the channel estimation results to [10] and [17], we use $K = 2$, the maximum number of measurements of $q_{\max} = 264$ and the target PEE set to 10^{-2} for all the algorithms.

B. The PEE performance

Achieving a target PEE is essential for guaranteeing a reliable communication between the TX and RX. Fig. 5 represents the probability of estimation error for different SNRs of the communication system. The results are compared to two prior works [10] and [17]. In [10], the authors only considered the channel estimation without a limit for PEE. As it can be seen in the figure, the algorithm cannot ensure that the probability of estimation error stays below the threshold of 10^{-2} . Therefore, this algorithm is used as a baseline in this figure and the main comparison is between [17] and our work. The figure indicates that both algorithms achieve the desired PEE with a negligible difference. Note that there is always a probability of outage in the system. This explains why in low SNR the PEE is over the predetermined threshold.

Furthermore, we approximate PEE of the RAF algorithm by deriving a closed-form lower bound and upper bound. Looking at the problem from information theory perspective, we are encoding a vector v entailing K^2 bits over q measurements using generator matrix $\mathbf{G}^{s,q}$. On the RX side, we are observing

the signal $\mathbf{c}^{s,q}$ from which we estimate the transmitted symbol (vector v). In stage s , assuming all the previous stages have been correct, we define the PEE as

$$p(EE|\mathbf{G}^{s,q}, v) = p(v \neq \hat{v}), \quad (57)$$

where by EE we refer to estimation error and $p(v \neq \hat{v})$ indicates the probability of an event in which the estimated vector \hat{v} is not equal to the transmitted vector v . This probability can be written in terms of the union of possible outcomes as

$$p(v \neq \hat{v}) = \bigcup_{\hat{v} \in \mathcal{V}, v \neq \hat{v}} p(\mathbf{c}^{s,q} \rightarrow \hat{\mathbf{c}}^{s,q}). \quad (58)$$

Where $\hat{\mathbf{c}}^{s,q}$ is the observation vector corresponding to \hat{v} and the term $p(\mathbf{c}^{s,q} \rightarrow \hat{\mathbf{c}}^{s,q})$ indicates the probability of an event in which $\hat{\mathbf{c}}^{s,q}$ is chosen as the outcome over $\mathbf{c}^{s,q}$. As we are using maximum likelihood method to detect the received symbol, referencing to [4], the pairwise probability of error estimation over the fading channel with channel coefficient of $\alpha \sim \mathcal{N}(0, Q)$ can be calculated as

$$p(\mathbf{c}^{s,q} \rightarrow \hat{\mathbf{c}}^{s,q}) = 0.5 - \sqrt{\frac{\Omega^2}{8 + 4\Omega^2}}, \quad (59)$$

where Ω is given as

$$\Omega = \sqrt{\frac{PQC_s^4}{2N_0}} \|\mathbf{G}^{s,q}(\mathbf{v} - \hat{\mathbf{v}})\|^2. \quad (60)$$

Having the pairwise probability of error estimation and conditioning on the transmitted vector v , PEE for the given generator matrix can be written as

$$p(EE|\mathbf{G}^{s,q}) = \sum_{v \in \mathcal{V}} p(v) p(EE|\mathbf{G}^{s,q}, v) \quad (61)$$

$$= \sum_{v \in \mathcal{V}} p(v) \bigcup_{\hat{v} \in \mathcal{V}, v \neq \hat{v}} p(\mathbf{c}^{s,q} \rightarrow \hat{\mathbf{c}}^{s,q}) \quad (62)$$

$$= \sum_{v \in \mathcal{V}} p(v) \bigcup_{\hat{v} \in \mathcal{V}, v \neq \hat{v}} \left(.5 - \sqrt{\frac{\Omega^2}{8 + 4\Omega^2}} \right). \quad (63)$$

An upper bound for equation (63) can be found by replacing union with summation which results in

$$p(EE|\mathbf{G}^{s,q}) \leq \sum_{v \in \mathcal{V}} \sum_{\substack{\hat{v} \in \mathcal{V} \\ v \neq \hat{v}}} p(v) \left(.5 - \sqrt{\frac{\Omega^2}{8 + 4\Omega^2}} \right). \quad (64)$$

Based on equation (64) an upper bound for the PEE over all stages 1 to S can be calculated as

$$p(EE) = 1 - \prod_{s=1}^S (1 - p(EE|\mathbf{G}^{s,q})) \quad (65)$$

$$\leq \sum_{s=1}^S \sum_{v \in \mathcal{V}} \sum_{\substack{\hat{v} \in \mathcal{V} \\ v \neq \hat{v}}} p(v) \left(.5 - \sqrt{\frac{\Omega^2}{8 + 4\Omega^2}} \right). \quad (66)$$

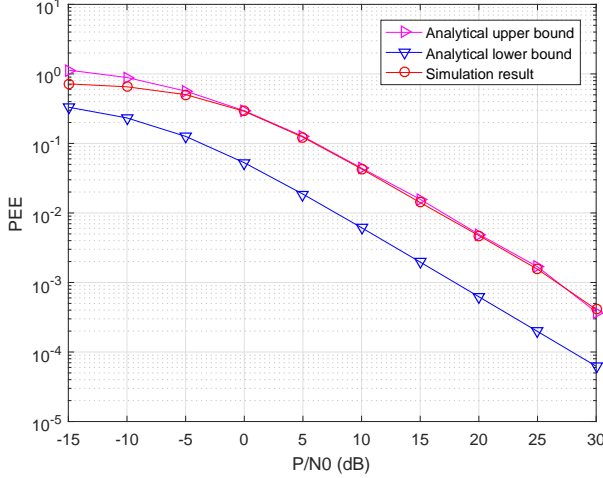


Figure 6: Comparison of the numerical and analytical results for PEE.

Also, assuming that all the possible realization of the set \mathcal{V} have equal probability a lower bound for PEE can be derived as

$$p(EE|\mathbf{G}^{s,q}) \geq .5 - \sqrt{\frac{PQC_s^4 \|\mathbf{v} - \hat{\mathbf{v}}\|^2}{16N_0 + PQC_s^4 \|\mathbf{v} - \hat{\mathbf{v}}\|^2}}. \quad (67)$$

Fig. 6 represents the comparison of the derived expressions and numerical results.

C. Overall Duration of the Channel Estimation

The main consideration in the effectiveness of the channel estimation algorithms is the overall time required for channel estimation. This criterion is crucial since anytime left will be assigned to data transmission. The following paragraphs show why the RAF algorithm significantly reduces the channel estimation period.

Each pilot transmission requires one time slot. On the other hand, each feedback bit also transmitted in one time slot. Therefore, the overall time of the channel estimation is the sum of these two numbers. Hence, in order to calculate the duration of channel estimation, these two factors need to be studied. Recall that the algorithms are ensuring the PEE in addition to channel estimation. Thus, we do not consider the channel estimation algorithm in [10]. We focus on comparing our results in terms of feedback overhead and pilot transmissions (measurements) with prior work in [17]. Fig. 7 exhibits the performance of the algorithms with regard to the number of feedback bits they need. It can be seen that the RAF algorithm requires a significantly low number of feedback bits. The average feedback bits required is almost as low as the optimal number. The difference between the algorithms becomes apparent, particularly in low SNR regime.

The trade-off between the number of measurements and feedback overhead is illustrated in Fig. 8. It is clear to see that the reduction in feedback bits is much higher than the increase of pilot transmissions required for the channel estimation. On average, the feedback reduction is 75.5%, whereas the

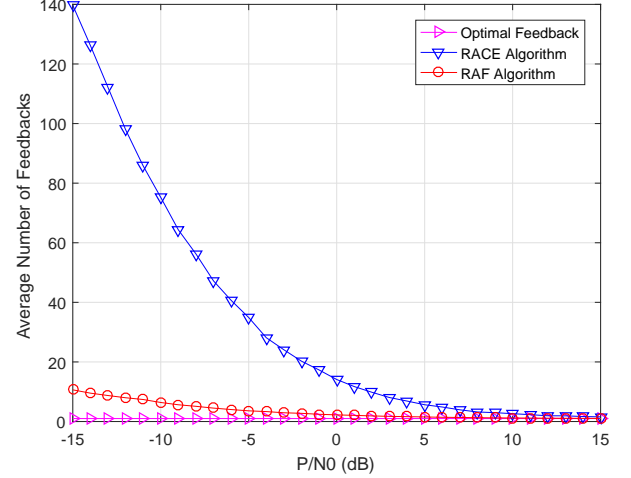


Figure 7: Feedback performance of the RAF algorithm compared to [17] and the optimal number of feedback bits.

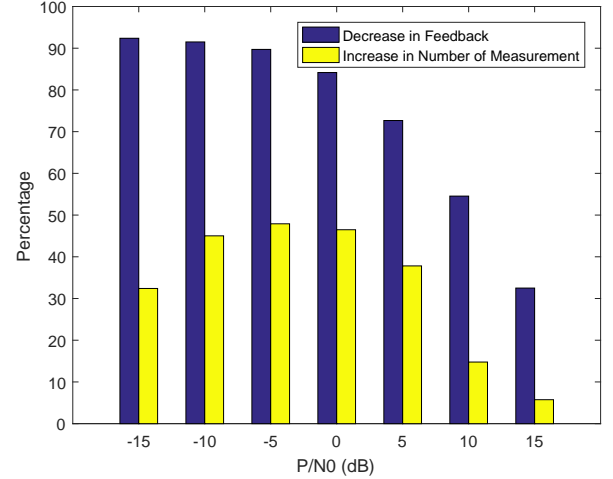


Figure 8: Change in the performance of the RAF algorithm in comparison with [17]. The graph explains the trade-off between the rise in the average number of measurements and feedback bits reduction.

increase in the number of measurement is only 34.4%. The overall time of the channel estimation in each stage of the algorithms is shown in Fig. 9. This figure illustrates the superior performance of the RAF algorithm. On average, for SNRs from -15dB to 15dB, the performance improves by 14%. At low SNRs, the difference is more significant. For instance, in an SNR of -15dB, the overall time required for the channel estimation is reduced by 30% using the RAF algorithm.

D. Performance Results of the Proposed Beam Tracking

Fig. 10 shows the sample tracking performance of the vehicle in terms of the state variables, velocity and position. The main factors affecting the tracking performance are the received SNR and the number of antennas used at the TX and RX. The mean square error (MSE) performance of the EKF

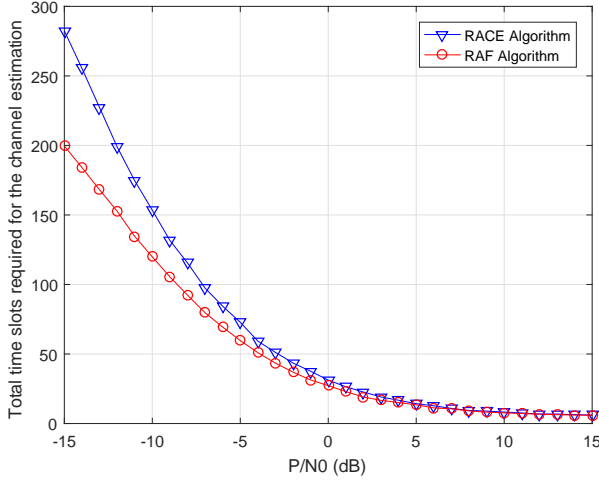


Figure 9: Comparison of the time required for the channel estimation in each stage.

tracking algorithm for various SNRs over 3000 experiments is shown in Fig. 11. The performance is shown for the AoD, similarly, it can be shown for AoA as they are both functions of the position. The valid tracking threshold is chosen to be $\sqrt{E[|\phi_m - \bar{\phi}_m|^2]} = BW/2$ [29], where BW denotes the half power beamwidth of the antenna array. Therefore, we define that the tracking is lost if the MSE is larger than a threshold. Such threshold is indicated by a horizontal line on the graphs. Note that half power beamwidth is a function of the beam direction, it is maximum for the end-fire direction and minimum for the broadside direction [33]. Logically, we choose the broadside direction as our threshold so that our results stay valid in the other scenarios as well. The broadside direction of the beam happens when the vehicle is exactly below the antenna array and its value can be estimated as $\frac{\lambda}{dN}$. Considering Fig. 11, the plots at the SNR = -5, 0, 5 dB cross the threshold in 24, 31 and 38 transmission blocks duration, respectively (each transmission block corresponds to 1ms). As expected, by increasing the SNR, the valid duration of the beam tracking improves. Moreover, Table I provides a comparison table for the various SNRs and number of antennas. The overall trend indicates that by increasing the number of antennas, as the beams get narrower, the valid duration of tracking decreases.

Table I: Valid tracking duration (in terms of transmission blocks) for different SNRs based on number of antennas

	Threshold	SNR = -5 dB	SNR = 0 dB	SNR = 5 dB
$N = 16$	0.0039	77	105	135
$N = 32$	0.0010	51	62	75
$N = 64$	0.0002	24	31	38
$N = 128$	0.0001	17	18	20

The most relevant prior work to our scheme is the one proposed in [29]. The authors used AoA, AoD and the channel coefficient as their state variables. It was assumed that the angles evolve using a process noise with zero mean and variance

of $(\frac{.5}{180}\pi)^2$ which is not able to characterize how a vehicle moves in the real world as we derived in this paper. The result of the comparison is shown in Fig. 12. The number of antennas is set to sixteen for a fair comparison with the previous work. Since our proposed model considers the dynamics of the system, the valid tracking duration is increased from 85 transmission blocks to 105 transmission blocks. It must be mentioned that the model in [29] did not consider realistic factors such as the velocity of the vehicle, block duration, etc. As addressed in this paper, if angles are used as state variables for the movement of the vehicle, the state evolution model is no longer a linear one. Such non-linearity leads to a high complexity in the calculation of Jacobians, which cannot be easily implemented in practical mmWave vehicular networks. Another important factor that was not considered in [29] is the number of antennas used at transceivers. This number was set to sixteen, irrespective of consequences that larger antenna arrays may cause. In practice, mmWave communication systems are likely to have large antenna arrays to compensate for the path loss which is more significant in shorter wavelengths. Table II indicates the valid tracking duration of the previous work compared to our proposed model for the various number of antennas. It can be seen that increasing the number of antennas significantly deteriorates the valid duration of the beam tracking. For instance, once equipping the transceivers with sixty-four antennas, the previous model can only track the user on average for 4 successive transmission blocks whereas our proposed model can extend the tracking duration on average to 31 transmission blocks. To sum up, considering the dynamics of the vehicular communication, our proposed model is able to improve the tracking period significantly in comparison to the existing methods.

Table II: Comparison of the valid tracking duration (in terms of transmission blocks) for different number of antennas at SNR = 0dB

	$N = 16$	$N = 32$	$N = 64$	$N = 128$
Prior model in [29]	85	19	4	3
Our proposed model	105	62	31	8
Improvement	20	43	27	15

Ultimately, after considering the performance of the RAF channel estimation algorithm and the proposed model for beam tracking, we investigate the impact of the channel estimation error on the tracking performance of the vehicle. Fig. 13 demonstrates how inaccurate channel estimation can lead to a decrease in the valid duration of beam tracking. For the purpose of demonstration, in this figure, the number of antennas is set to 16 and the channel estimation errors are chosen based on the half power beamwidth which as before calculated as $BW = \frac{\lambda}{dN}$. The maximum possible error ($BW/2$) is divided to four equal divisions and the result of 3000 runs of each is illustrated in the figure. The summary of the valid tracking duration for each of the errors is given in Table III. It is evident from the table that larger estimation

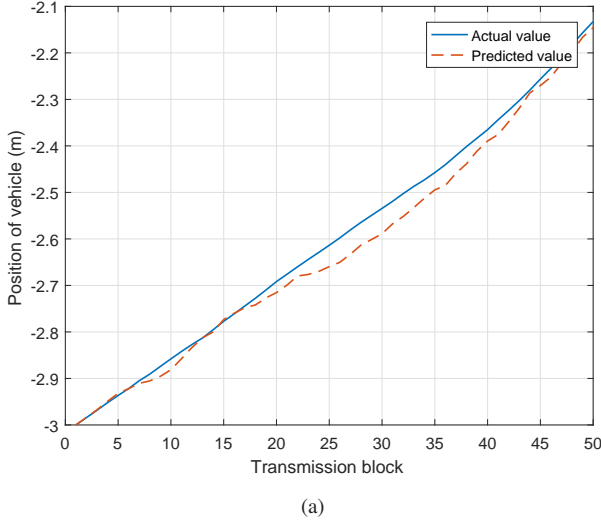


Figure 10: Sample tracking performance of the EKF for a moving vehicle in terms of the state variables, velocity and position at SNR = 0.

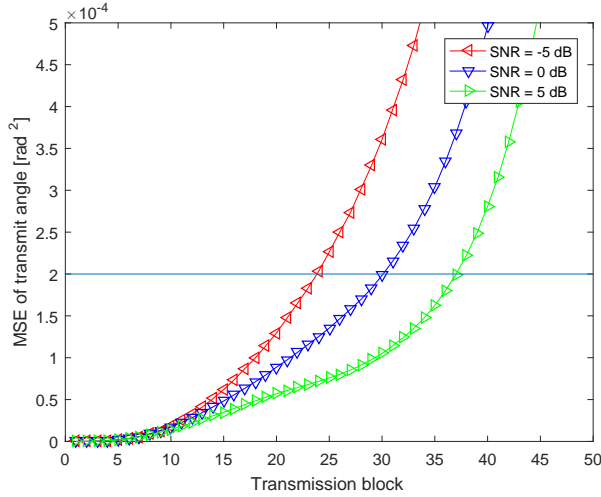


Figure 11: Effect of SNR on tracking performance of the EKF.

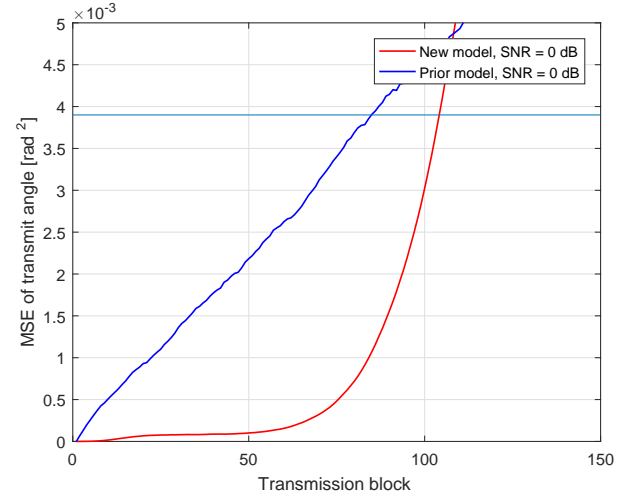


Figure 12: Comparison of the proposed model for vehicular communication to the prior work in [29].

error directly deteriorates the performance of the tracking. Therefore, having a robust algorithm such as RAF is necessary to ensure that the probability of estimation error is below an acceptable threshold according to the system requirements.

Table III: Impact of channel estimation error on beam tracking performance at SNR=0dB (in terms of transmission blocks)

Channel estimation error	0	$\frac{BW}{8}$	$\frac{BW}{4}$	$\frac{3BW}{8}$	$\frac{BW}{2}$
Valid tracking duration	105	93	85	72	64

VI. CONCLUSION

In this paper, we have proposed a framework consisting of channel estimation and beam tracking for mmWave vehicular to infrastructure communications. The proposed RAF

algorithm can reduce the high overhead of channel estimation feedback in the existing algorithms. Simulation results indicate that the algorithm can reduce the time required for the channel estimation by 14% and the feedback overhead by 75.5% on average. We have also investigated the implementation of the EKF beam tracking for mmWave vehicular communications. New state evolution and observation models have been proposed considering the vehicle's position, the vehicle's velocity, and the channel coefficient.

REFERENCES

- [1] "Cisco visual networking index: Global mobile data traffic forecast update, 2016–2021 white paper," Mar 2017. [Online]. Available: <https://www.cisco.com/c/en/us/solutions/collateral/service-provider/visual-networking-index/>

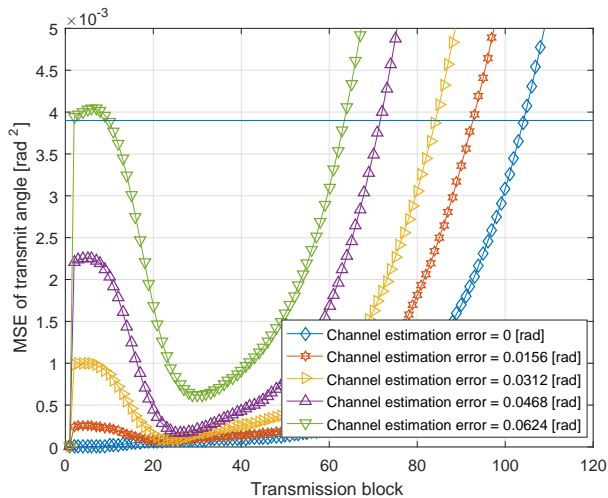


Figure 13: Effect of channel estimation error on the proposed model for beam tracking.

- [2] T. S. Rappaport, S. Sun, R. Mayzus, H. Zhao, Y. Azar, K. Wang, G. N. Wong, J. K. Schulz, M. Sanimi, and F. Gutierrez, "Millimeter wave mobile communications for 5g cellular: It will work!" *IEEE Access*, vol. 1, pp. 335–349, 2013.
- [3] Z. Pi and F. Khan, "An introduction to millimeter-wave mobile broadband systems," *IEEE Communications Magazine*, vol. 49, no. 6, pp. 101–107, June 2011.
- [4] R. Van Nobelen and D. P. Taylor, "Analysis of the pairwise error probability of noninterleaved codes on the rayleigh-fading channel," *IEEE transactions on communications*, vol. 44, no. 4, pp. 456–463, 1996.
- [5] H. Rate, "Ghz phy, mac and hdmi pal," 2008.
- [6] "Ieee 802.15 wpan." [Online]. Available: <http://www.ieee802.org/15/pub/TG3c.html>
- [7] E. Ferro and F. Potorti, "Bluetooth and wi-fi wireless protocols: a survey and a comparison," *IEEE Wireless Communications*, vol. 12, no. 1, pp. 12–26, 2005.
- [8] A. Kato, K. SATO, M. Fujise, and S. KAWAKAMI, "Propagation characteristics of 60-ghz millimeter waves for its inter-vehicle communications," *IEICE transactions on communications*, vol. 84, no. 9, pp. 2530–2539, 2001.
- [9] H. T. Friis, "A note on a simple transmission formula," *Proceedings of the IRE*, vol. 34, no. 5, pp. 254–256, May 1946.
- [10] A. Alkhateeb, O. E. Ayach, G. Leus, and R. W. Heath, "Channel estimation and hybrid precoding for millimeter wave cellular systems," *IEEE Journal of Selected Topics in Signal Processing*, vol. 8, no. 5, pp. 831–846, Oct 2014.
- [11] O. El Ayach, S. Rajagopal, S. Abu-Surra, Z. Pi, and R. W. Heath, "Spatially sparse precoding in millimeter wave mimo systems," *IEEE transactions on wireless communications*, vol. 13, no. 3, pp. 1499–1513, 2014.
- [12] R. Méndez-Rial, C. Rusu, N. González-Prelcic, A. Alkhateeb, and R. W. Heath, "Hybrid mimo architectures for millimeter wave communications: Phase shifters or switches?" *IEEE Access*, vol. 4, pp. 247–267, 2016.
- [13] G. R. MacCartney and T. S. Rappaport, "73 ghz millimeter wave propagation measurements for outdoor urban mobile and backhaul communications in new york city," in *2014 IEEE International Conference on Communications (ICC)*, June 2014, pp. 4862–4867.
- [14] A. Alkhateeb, G. Leus, and R. W. Heath, "Compressed sensing based multi-user millimeter wave systems: How many measurements are needed?" in *2015 IEEE International Conference on Acoustics, Speech and Signal Processing (ICASSP)*, April 2015, pp. 2909–2913.
- [15] S. Hur, T. Kim, D. J. Love, J. V. Krogmeier, T. A. Thomas, and A. Ghosh, "Millimeter wave beamforming for wireless backhaul and access in small cell networks," *IEEE Transactions on Communications*, vol. 61, no. 10, pp. 4391–4403, October 2013.
- [16] M. Kokshoorn, H. Chen, P. Wang, Y. Li, and B. Vucetic, "Millimeter wave mimo channel estimation using overlapped beam patterns and rate adaptation," *IEEE Transactions on Signal Processing*, vol. 65, no. 3, pp. 601–616, Feb 2017.
- [17] M. Kokshoorn, H. Chen, Y. Li, and B. Vucetic, "Race: A rate adaptive channel estimation approach for millimeter wave mimo systems," in *2016 IEEE Global Communications Conference (GLOBECOM)*, Dec 2016, pp. 1–6.
- [18] K. Hosoya, N. Prasad, K. Ramachandran, N. Orihashi, S. Kishimoto, S. Rangarajan, and K. Maruhashi, "Multiple sector id capture (midc): A novel beamforming technique for 60-ghz band multi-gbps wlan/pan systems," *IEEE Transactions on Antennas and Propagation*, vol. 63, no. 1, pp. 81–96, Jan 2015.
- [19] Y. Inoue, Y. Kishiyama, Y. Okumura, J. Kepler, and M. Cudak, "Experimental evaluation of downlink transmission and beam tracking performance for 5g mmw radio access in indoor shielded environment," in *2015 IEEE 26th Annual International Symposium on Personal, Indoor, and Mobile Radio Communications (PIMRC)*, Aug 2015, pp. 862–866.
- [20] C. Zhang, D. Guo, and P. Fan, "Tracking angles of departure and arrival in a mobile millimeter wave channel," in *2016 IEEE International Conference on Communications (ICC)*, May 2016, pp. 1–6.
- [21] V. Va, H. Vikalo, and R. W. Heath, "Beam tracking for mobile millimeter wave communication systems," in *2016 IEEE Global Conference on Signal and Information Processing (GlobalSIP)*, Dec 2016, pp. 743–747.
- [22] X. Zhang, A. F. Molisch, and S.-Y. Kung, "Variable-phase-shift-based rf-baseband codesign for mimo antenna selection," *IEEE Transactions on Signal Processing*, vol. 53, no. 11, pp. 4091–4103, Nov 2005.
- [23] V. Venkateswaran and A. J. van der Veen, "Analog beamforming in mimo communications with phase shift networks and online channel estimation," *IEEE Transactions on Signal Processing*, vol. 58, no. 8, pp. 4131–4143, Aug 2010.
- [24] O. E. Ayach, S. Rajagopal, S. Abu-Surra, Z. Pi, and R. W. Heath, "Spatially sparse precoding in millimeter wave mimo systems," *IEEE Transactions on Wireless Communications*, vol. 13, no. 3, pp. 1499–1513, March 2014.
- [25] C. Balanis, "Antenna theory analysis and design, third edition ed," *United States of America: John Wiley Sons*, vol. 2005, 2005.
- [26] S. Han, C. I. I, Z. Xu, and C. Rowell, "Large-scale antenna systems with hybrid analog and digital beamforming for millimeter wave 5g," *IEEE Communications Magazine*, vol. 53, no. 1, pp. 186–194, January 2015.
- [27] L. Dai and X. Gao, "Prior-aided channel tracking for millimeter-wave beamspace massive mimo systems," in *2016 URSI Asia-Pacific Radio Science Conference (URSI AP-RASC)*, Aug 2016, pp. 1493–1496.
- [28] R. W. Heath, N. González-Prelcic, S. Rangan, W. Roh, and A. M. Sayeed, "An overview of signal processing techniques for millimeter wave mimo systems," *IEEE Journal of Selected Topics in Signal Processing*, vol. 10, no. 3, pp. 436–453, April 2016.
- [29] V. Va, H. Vikalo, and R. W. Heath, "Beam tracking for mobile millimeter wave communication systems," in *2016 IEEE Global Conference on Signal and Information Processing (GlobalSIP)*, Dec 2016, pp. 743–747.
- [30] C. E. Shannon, "A mathematical theory of communication," *The Bell System Technical Journal*, vol. 27, no. 3, pp. 379–423, July 1948.
- [31] J. Vince, *Geometric algebra for computer graphics*. Springer Science & Business Media, 2008.
- [32] T. Kailath, A. H. Sayed, and B. Hassibi, *Linear estimation*. Prentice Hall Upper Saddle River, NJ, 2000, vol. 1.
- [33] W. L. Stutzman and G. A. Thiele, *Antenna theory and design*. John Wiley & Sons, 2012.